Physica B 406 (2011) 1818–1821

Contents lists available at ScienceDirect

Physica B

journal homepage: www.elsevier.com/locate/physb

P–n codoping induced enhancement of ferromagnetism in Mn-doped In_2O_3: A first-principles study

Wen-Yan Ke [a], Shi-Fei Qi [a,*], Yu-Jun Zhao [b], Xiao-Hong Xu [a]

[a] School of Chemistry and Materials Science, Shanxi Normal University, Linfen 041004, People's Republic of China
[b] Department of Physics, South China University of Technology, Guangzhou 510640, People's Republic of China

ARTICLE INFO

Article history:
Received 5 November 2010
Accepted 11 February 2011
Available online 17 February 2011

Keywords:
Diluted magnetic semiconductors
First-principles calculation
p–n codoping
Ferromagnetic stability

ABSTRACT

We have performed first-principles density functional theory calculation in order to investigate the feasibility of "*p–n* codoping method" in improving magnetic property of In_2O_3 based diluted magnetic semiconductors. We find that the ferromagnetic state is favored in Mn-doped In_2O_3, and Sn doping can increase magnetic moment in Mn-doped In_2O_3. These findings are in line with our earlier experimental observation. Along with previous works, we now have enough evidences to support that *p–n* codoping is a valid method to improve magnetism of oxides based diluted magnetic semiconductors.

1. Introduction

Diluted magnetic semiconductors (DMS) have attracted much attention for their potential applications in the field of spintronics [1–3]. Such applications require the DMSs to be ferromagnetic above room temperature. Despite the very obvious progress in developing DMSs, many important issues such as the origin of FM ordering [4–10], the solubility of dopant [11,12], and low Curie temperature [13,14], which arise from the study of this unique class of disordered magnetic system still exist [3].

In the DMS study, Xu et al. performed the experimental study of Mn/Al codoped ZnO and found that the magnetism of researched system could be largely improved [15]. Latterly, Zhang et al. theoretically investigated Mn/P codoped Si [16,17], Mn/As codoped Ge [16,17], and Cr/N codoped TiO_2 [18]. Their series of studies confirmed that such codoping may decrease the appearance of interstitial dopant, increase the solubility of dopant, improve the magnetism, and enhance the visible-light photoactivity [15–18]. In fact, above codopings have a common character of simultaneously incorporating *p*- and *n*-type dopants into semiconductors. Hence, such codoping is named as *p–n* codoping. In *p–n* codoping, the columbic attraction between the *p*- and *n*-type dopants with opposite charge state substantially enhances both the thermodynamic and, in particular, the kinetic solubilities of the dopant pairs in concerted substitutional doping [16–18]. It is concluded that the *p–n* codoping concept may be a powerful guiding principle in future design of various functional materials [15,16–19].

In this paper, we theoretically study the feasibility of *p–n* codoping method in improving magnetic property of In_2O_3 based diluted magnetic semiconductors. Our calculations show that the ferromagnetic coupling is favored in Mn-doped In_2O_3. Then, it is found that Sn doping can increase the moment in Mn-doped In_2O_3. This finding agrees with our recent experimental observation. Along with previous works [15–18], *p–n* codoping is demonstrated to be a valid method to improve magnetism of Si, Ge, ZnO, and In_2O_3 based diluted magnetic semiconductors.

2. Computational details

The first-principles calculations were performed within the framework of the density functional theory (DFT), using the projector-augmented wave (PAW) [20] method as implemented in the VASP code [21–23]. We adopted the generalized gradient approximation (GGA-PBE) [24] for treating the exchange correlation interaction. The atomic structures were fully optimized until the Hellmann–Feynman forces on each ion were less than 0.02 eV/Å. A plane-wave energy cut-off of 500 eV, a $3\times3\times3$ k-points grid, and the Gaussian smearing method with a 0.1 eV smearing width were used in the structure relaxation. A k-point grid of $4\times4\times4$ is applied for the final total energy calculations at the equilibrium volume. Our model is similar to that of recent studies of TM-doped In_2O_3 system [25,26]. As shown in Fig. 1, two extra Mn are introduced in an 80-atom In_2O_3 supercell, corresponding to 6.25% Mn, comparable to the concentration in our experiments [27]. In the present calculations, we fix one dopant

* Corresponding author.
E-mail address: qishifei@yahoo.com.cn (S.-F. Qi).

0921-4526/$ - see front matter © 2011 Elsevier B.V. All rights reserved.
doi:10.1016/j.physb.2011.02.036

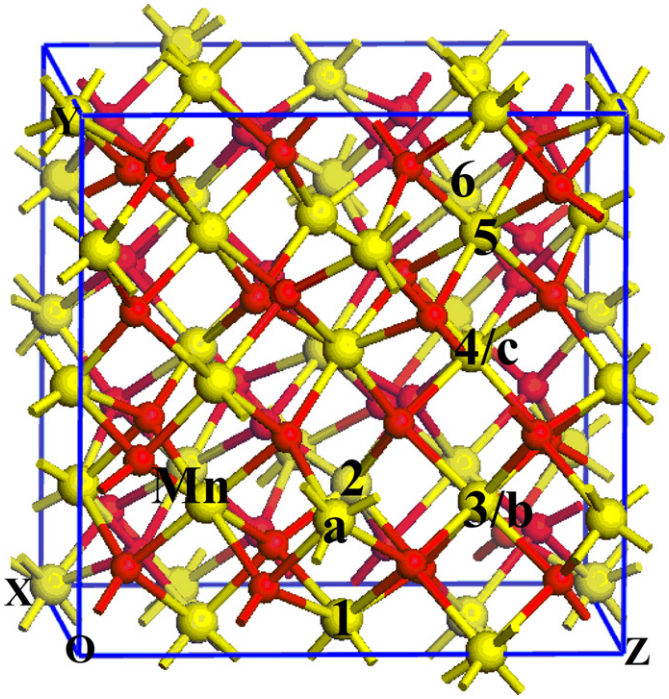

Fig. 1. 80-atom supercell of In_2O_3. Red (small) and yellow (big) balls represent O and In atoms, respectively. In our study, one Mn is fixed at the position of labeled Mn, and the other one locates at the positions labeled with 1, 2, 3, 4, 5, and 6 in different configurations. The positions of Sn dopant are labeled with *a*, *b*, and *c* in different configurations. (For interpretation of the references to color in this figure legend, the reader is referred to the web version of this article.)

Mn atom (denoted as Mn in Fig. 1) and vary the positions of the second Mn atom (denoted as 1, 2, 3, 4, 5, and 6) to obtain different configurations. Some configurations are further doped with an additional Sn atom. The variation of Sn position (denoted as *a*, *b*, or *c*) is also considered as a function of the separation distance to the two Mn atoms.

3. Results and discussion

At first, we discuss the most stable structures and magnetic property of Mn-doped In_2O_3 (IMO). Fig. 2 presents the variation of total energies of ferromagnetic (FM) and antiferromagnetic (AFM) states as a function of Mn–Mn separation distance. From it, we can find that the FM and AFM stabilities generally decrease as Mn–Mn distance increases, indicating that Mn ions prefer to accumulate together in the Mn-doped In_2O_3. This is consistent with the observation in Fe-doped In_2O_3 [25]. It is noted that the total energies of FM states in the configurations 1 and 2 (respectively denoted as 1-IMO and 2-IMO) are similar to each other. Hence, the 1-IMO and 2-IMO are the most energetically favorable structures. Fig. 2 and Table 1 also show that the FM spin ordering predominates over the exchange interaction for all the studied configurations except the configuration 4, where the FM and AFM states are degenerated. The calculated FM stability in Mn-doped In_2O_3 is in good agreement with our recent experimental observation [27].

Next, we consider the effect of adding Sn on the magnetic properties of Mn-doped In_2O_3. As shown in Fig. 1, by substituting Sn for an In atom at the site *a* near Mn–Mn and *c* far from Mn–Mn in configuration 1 (1-IMO), we obtain two configurations of Mn/Sn codoped In_2O_3. They are denoted by 1-IMSO-*a* and 1-IMSO-*c*. Similarly, we can obtain the 2-IMSO-*b* (near Mn–Mn) and 2-IMSO-*c* (far from Mn–Mn) based on the stable configuration 2 in Mn-doped In_2O_3. the calculated ΔE_{FM-AFM} of 1-IMSO-*a*, 2-IMSO-*b*, and 2-IMSO-*c* are −34, −13, and −39 meV, respectively, as listed in Table 1. For the 1-IMSO-*a*, the exchange energy ΔE_{FM-AFM} was not obtained since its AFM state was converged to ferrimagnetic state spontaneously in our calculations. Hence, no ΔE_{FM-AFM} value of 1-IMSO-*c* is listed in the Table 1. All the calculated ΔE_{FM-AFM} are negative, indicating that the ground state is FM for all the studied configurations. Of note, the 2-IMSO-*b* and 2-IMSO-*c* are more stable than 1-IMSO-*a* and 1-IMSO-*b* configurations.

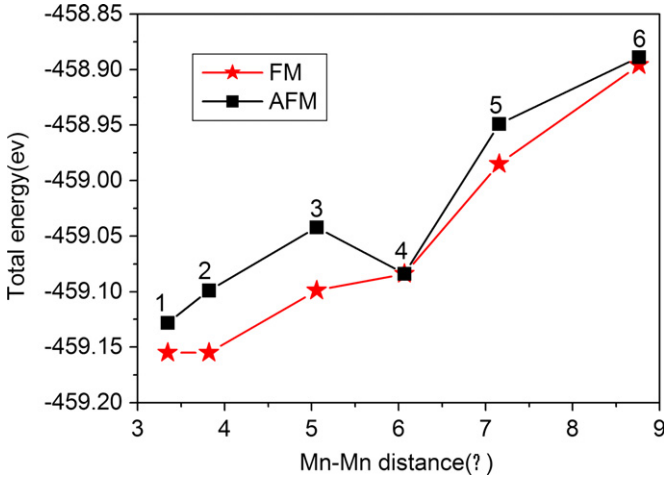

Fig. 2. Variation of total energies of ferromagnetic (FM) and antiferromagnetic (AFM) states as a function of Mn–Mn separation distance in Mn-doped In_2O_3.

Table 1
Calculated results of Mn and Mn/Sn codoped In_2O_3 systems. Total energy (E_{total}), the difference of FM and AFM states (ΔE_{FM-AFM}), and total moment (M_{total}) are summarized.

Configuration	E_{total} (eV)		ΔE_{FM-AFM} (meV)	M_{total} (μB)	
	FM	AFM		FM	AFM
1-IMO	−459.155	−459.128	−27	7.590	0.000
2-IMO	−459.155	−459.099	−56	7.834	0.000
3-IMO	−459.099	−459.042	−57	7.635	0.000
4-IMO	−459.084	−459.084	0	7.610	−0.395
5-IMO	−458.985	−458.949	−36	7.684	0.000
6-IMO	−458.896	−458.889	−7	7.437	0.000
1-IMSO-*a*	−460.485	−460.451	−34	8.414	−0.442
1-IMSO-*c*	−460.399	−460.303[a]	–	8.097	–
2-IMSO-*b*	−460.583	−460.570	−13	8.480	0.341
2-IMSO-*c*	−460.532	−460.493	−39	8.369	0.188

[a] Energy of ferrimagnetic state. AFM state is not stable in our calculation.

The total magnetic moment of the Mn and Mn/Sn codoped In_2O_3 systems are also listed in Table 1. We can find that the Sn doping greatly enhances the total moments compared with the case of Mn-doped In_2O_3. For example, the total moment of 2-IMSO-*c* is 8.369μB, which is larger than that of 2-IMO, 7.834μB. This finding has been supported by our recent experimental observation that moment of Mn/Sn codoped In_2O_3 sample becomes larger than that of Mn-doped In_2O_3 sample [27].

The above results have shown that Sn doping can increase moment in Mn-doped In_2O_3. Deeper understanding of above results requires a careful examination of the microscopic coupling mechanism. We first inspect the differences of electronic structure in Mn-doped In_2O_3 with and without Sn doping.

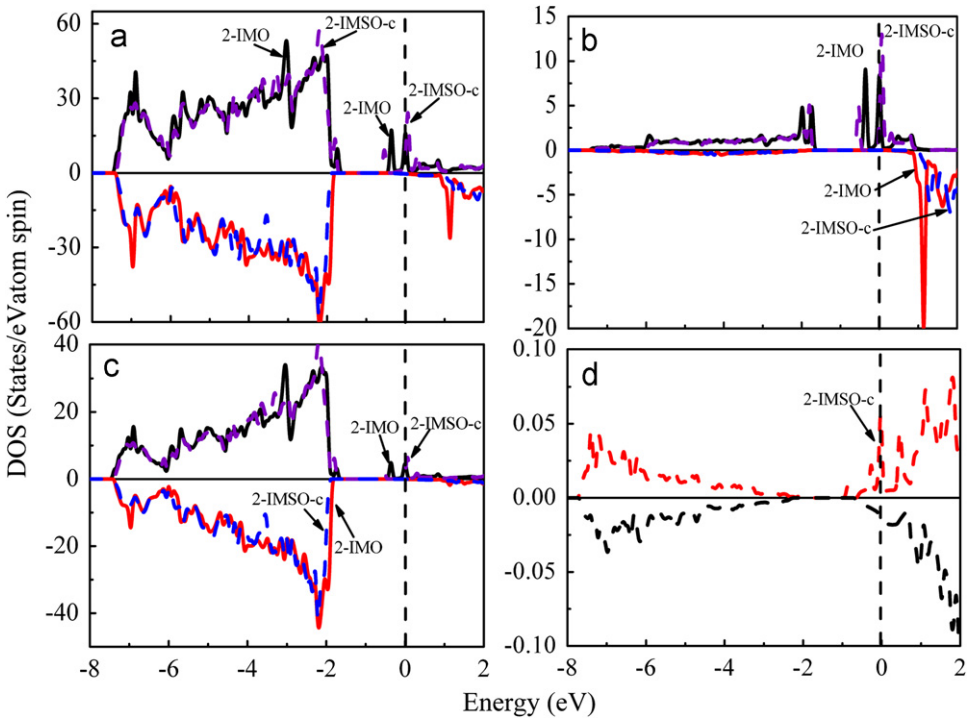

Fig. 3. TDOSs and PDOSs of Mn 3d, O 2p and Sn 5*s* for the Mn (sold lines) and Mn/Sn (dash lines) codoped In_2O_3 systems in FM ordering. Fermi energy is set to zero. (a) TDOS, (b) Mn-3d-PDOS, (c) O-2p-PDOS and (d) Sn-55-PDOS.

Fig. 3(a)–(d) presents the density of states (DOS) spectra of 2-IMO and 2-IMSO-*c* with FM ordering. For the 2-IMO, Mn 3d and O 2p are clearly hybridized, especially the O atoms in the surrounding of Mn atoms. The hybridization between the Mn atoms and their surrounding O atoms induced significant net magnetic moments on these oxygen atoms. Therefore, the total magnetic moments are mainly contributed by the dopants and neighboring O anions in Mn-doped In_2O_3. Above analysis also can be found from Fig. 4(a). With the codoping of Sn, it can be found that a new hybridization from Mn 3d, O 2p and Sn 5s appears, and this new hybridization leads to more obvious spin polarization around E_F. On the other hand, more Mn 3d major states, as displayed in Fig. 3(b) and (d), are occupied by electrons from Sn 5s due to the new hybridization, which may change the valence state of Mn from Mn^{3+} to Mn^{2+}. Bader's charge analysis also shows that the occupations of two Mn atoms are 4.796 and 4.821*e*, respectively in Mn-doped In_2O_3, while they become 4.803 and 4.834*e* in Mn/Sn codoped In_2O_3. Thus, compared with Mn-doped In_2O_3, the Sn doping increases the total moments of Mn-doped In_2O_3.

Then, we will discuss the FM coupling mechanism in Mn and Mn/Sn codoped In_2O_3. Fig. 2(a) and (b) shows the space distribution of spin density in 2-IMO and 2-IMSO-*c*, respectively. For the 2-IMO and 2-IMSO-*c*, Fig. 2(a) and (b) obviously indicates that two Mn ions produce FM coupling by the superexchange of bridging oxygen ions. The Mn cations and some of the surrounding O anions have larger spin polarizations in the 2-IMSO-*c* than those in the 2-IMO. This is in agreement with the earlier analysis of corresponding DOS. Therefore, it is believed that the ferromagnetism of Mn/Sn codoped In_2O_3 is enhanced than that of Mn-doped In_2O_3. This conclusion agrees with our recent experimental observation that Sn doping enhances magnetism of Mn/Sn codoped In_2O_3 sample [27]. It is also mentioned that the spin polarization in the Mn and Mn/Sn codoped In_2O_3 is highly anisotropic as evidenced by the spin density shown in the Fig. 2(a) and (b). Similar phenomenon was also reported in the Fe/Cu codoped In_2O_3 [25].

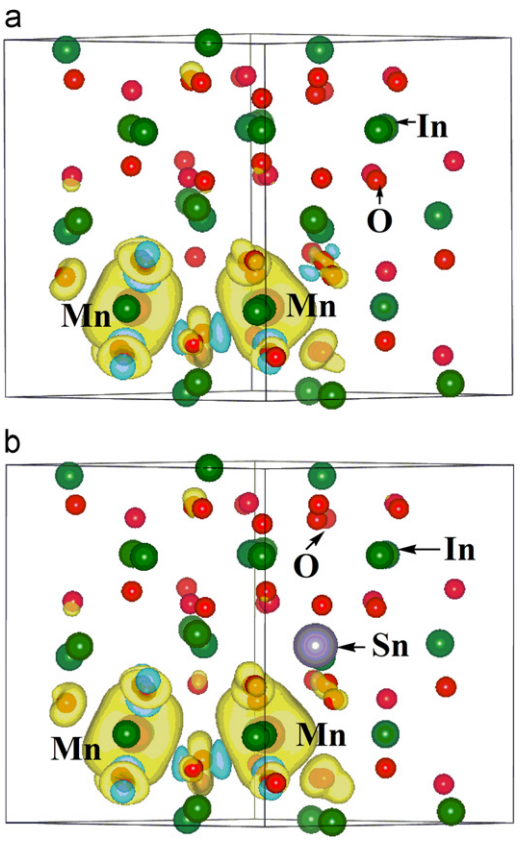

Fig. 4. Spin density distribution in the (a) Mn and (b) Mn/Sn codoped In_2O_3 systems in FM ordering. The yellow and blue isosurfaces correspond to the majority- and minority-spin density. The red, green, purple, and gray balls represent O, In, Mn, and Sn atoms, respectively. (For interpretation of the references to color in this figure legend, the reader is referred to the web version of this article.)

4. Conclusions

In summary, we have systematically studied the feasibility of "*p*–*n* codoping method" in improving magnetic property of In_2O_3 based diluted magnetic semiconductors by first-principles calculations. It has been demonstrated that in Mn-doped In_2O_3, the FM ordering is favored. By additional Sn doping, the total moment in all the studied Mn-doped In_2O_3 configurations can be enhanced, indicating that the *p*–*n* codoping is a valid method to improve magnetism of In_2O_3 based diluted magnetic semiconductors. Further electronic structure analysis reveals that the superexchange mechanism is responsible for the magnetic interaction of Mn and Mn/Sn codoped In_2O_3. Above theoretical findings are supported by our recent experimental observations.

Acknowledgements

This work was supported by the National Science Foundation for Distinguished Young Scholars (no. 51025101), the 863 Program (no. 2009AA03Z446), the NSFC (nos. 10574085 and 60776008), and NCET-07-0527 and NSFSX (nos. 2007021022, 2008011042-1, and 2009021014).

References

[1] I. Zutic, J. Fabian, S.Das Sarma, Rev. Mod. Phys. 76 (2004) 323.
[2] T. Jungwirth, J. Sinova, J. Masek, J. Kucera, A.H. MacDonld, Rev. Mod. Phys. 78 (2006) 809.
[3] F. Pan, C. Song, X.J. Liu, Y.C. Yang, F. Zeng, Mater. Sci. Eng. R 62 (2008) 1.
[4] A. Walsh, J.L.F. DaSilva, S.-H. Wei, Phys. Rev. Lett. 100 (2008) 256401.
[5] K. Sato, H.K. Yoshida, Jpn. J. Appl. Phys. 40 (2001) L334.
[6] T. Dietl, H. Ohno, F. Matsukura, J. Cibert, D. Ferrand, Science 287 (2000) 1019.
[7] M. Ruderman, C. Kittel, Phys. Rev. B 96 (1954) 99.
[8] D.M. Edwards, M.I. Katsnelson, J. Phys. C: Condens. Matter 18 (2006) 7209.
[9] J.M.D. Coey, M. Venkatesan, C.B. Fitzgerald, Nat. Mater. 4 (2005) 173.
[10] J.M.D. Coey, P. Stamenov, R.D. Gunning, M. Venkatesan, K. Paul, New J. Phys. 12 (2010) 053025.
[11] K. Ueda, H. Tabata, T. Kawai, Appl. Phys. Lett. 79 (2001) 988.
[12] J.H. Kim, H. Kim, D. Kim, Y.E. Ihm, W.K. Choo, Physica B 327 (2003) 304.
[13] S. von Molnar, D. Read, J. Magn. Magn. Mater. 13 (2002) 242.
[14] Y.D. Park, A.T. Hanbicki, S.C. Erwin, C.S. Hellberg, J.M. Sullivan, J.E. Mattson, T.F. Ambrose, A. Wilson, G. Spanos, B.T. Jonker, Science 295 (2001) 651.
[15] X.H. Xu, H.J. Blythe, M. Ziese1, A.J. Behan, J.R. Neal, A. Mokhtari, R.M. Ibrahim, A.M. Fox, G.A. Gehring, New J. Phys. 8 (2006) 135.
[16] W.G. Zhu, Z.Y. Zhang, E. Kaxiras, Phys. Rev. Lett. 100 (2008) 027205.
[17] H. Chen, W.G. Zhu, E. Kaxiras, Z.Y. Zhang, Phys. Rev. B 79 (2008) 235202.
[18] W.G. Zhu, X. Qiu, V. Iancu, X.-Q. Chen, H. Pan, N.M. Dimitrijevic, T. Rajh, H.M. Meyer III, M.P. Paranthaman, G.M. Stocks, H. Weitering, B. Gu, G. Eres, Z.Y. Zhang, Phys. Rev. Lett. 103 (2009) 226401.
[19] L.G. Wang, A. Zunger, Phys. Rev. Lett. 90 (2003) 256401.
[20] P.E. Blöchl, Phys. Rev. B 50 (1994) 17953.
[21] G. Kresse, J. Furthmuller, Comput. Mater. Sci. 6 (1996) 15.
[22] G. Kresse, J. Furthmuller, Phys. Rev. B 54 (1996) 11169.
[23] G. Kresse, S. Joubert, Phys. Rev. B 59 (1999) 1758.
[24] J.P. Perdew, K. Burke, M. Ernzerhof, Phys. Rev. Lett. 77 (2009) 3865.
[25] L.X. Guan, J.G. Tao, Z.R. Xiao, B.C. Zhao, X.F. Fan, C.H.A. Huan, J.L. Kuo, L. Wang, Phys. Rev. B 79 (2009) 184412.
[26] Z.R. Xiao, X.F. Fan, L.X. Guan, C.H.A. Huan, J.L. Kuo, L. Wang, J. Phys.: Condens. Matter 21 (2009) 272202.
[27] F.X. Jiang, X.H. Xu, J. Zhang, X.C. Fan, H.S. Wu, G.A. Gehring, Appl. Phys. Lett. 96 (2010) 052503.